

MEASURING SHIP UNDERWATER RADIATED NOISE IN SHALLOW WATERS - WHY NOT IN THE NEAR FIELD?

C Andersson IVL Swedish Environmental Research Institute
M Linné Swedish Defence Research Agency
T Johansson IVL Swedish Environmental Research Institute
M Andersson Swedish Defence Research Agency

1 INTRODUCTION

Measurements of underwater radiated noise (URN) from ships in shallow waters are subject to complications related to the wave interactions with the seabed. There is an ongoing scientific process to determine the best practice in terms of measurement geometry to use for this type of measurement, aiming to establish an ISO standard for shallow water measurements¹. One large contribution to this discussion is results from an investigation on various measurement geometries and propagation models². Their measurements show good agreement between deep water measurements and shallow water measurements when using a relatively simple propagation model. They also report better agreement for the hydrophones that they had closest to the ship track in horizontal arrays, and hydrophones closest to the bottom in vertical arrays. These configurations have in common that they have a large angle between the water surface and the line from the ship to the hydrophone (grazing angle). In their used hydrophone configurations, the highest grazing angle was around 10° for the site with depth of around 35 m and around 30° for the site with depth of around 66 m. Our current investigation is into how the results change when including hydrophones even closer to measure at higher grazing angles.

We measured the URN from a 11,000 GT chemical product tanker with an overall length of around 150 m in a dedicated measurement. The measurements took place outside the islet of Vinga in the Gothenburg archipelago, see section 2. To support the calculations of the ship source level, see section 4, the propagation loss was measured in the area, see section 3.

2 MEASUREMENT SITE AND GEOMETRY

The measurement site was situated approximately 1.7 km south-west of the islet of Vinga in the Gothenburg archipelago. The area has a quite flat bottom with a water depth of around 45 m, known to consist of mostly clay and mud. The ship source level measurements took place on the 30th of August 2023, whilst the propagation loss measurements took place one week later on the 6th of September. Both days were very calm with low wind speeds and wave heights below 0.5 m.

A total of eight hydrophones were used during the measurements, see table 1. The placement of these hydrophones were chosen with a combination of vertical arrays at distances longer than one ship length, as typically required by many deep-water measurement methods, and closer hydrophones to achieve the

Table 1: Placement of the eight hydrophones relative to the measurement track, and their deployment heights above the bottom.

Hydrophone	Distance from track	Height above bottom	Grazing angle
Colmar 1	-165 m	2 m	14.6°
Colmar 2	-165 m	12 m	11.3°
Sylence 1	0 m	2 m	90.0°
Sylence 2	220 m	2 m	11.1°
SoundTrap 1	35 m	2 m	50.9°
SoundTrap 2	70 m	2 m	31.6°
SoundTrap 3	70 m	20 m	19.7°
SoundTrap 4	220 m	15 m	7.8°

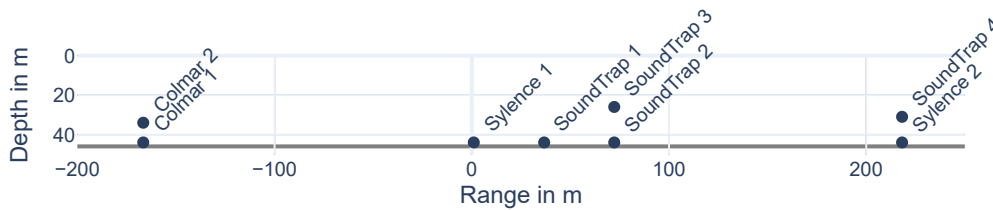


Figure 1: Measurement geometry with hydrophone placement.

higher grazing angles also desired in the same methods^{3,4,5}. An overview of the hydrophone placement can be seen in fig. 1.

3 PROPAGATION LOSS

During the propagation loss measurements, the cabled Colmar hydrophones and the furthest autonomous recorders (Sylence 2 and SoundTrap 4) were no longer deployed, hence the propagation loss measurements were performed with a subset of the hydrophones. A Lubell Labs model 1424 sound source was used to transmit a number of 4 s long linearly frequency-modulated chirps, one chirp each in the decade bands at 315 Hz, 630 Hz, 1 kHz, and 2 kHz. The chirps were sent from a drifting vessel, performing 5 runs through the measurement area. The weather was favorable, such that the drifting vessel had a similar trajectory as the measurement track for the source level measurements of the tanker. A reference hydrophone (Neptune D/70/H) was deployed at the same 4 m depth as the source at a horizontal distance of 5 m. A cross-correlation of the signal at the reference hydrophone and the input signal to the sound source was used to calculate the level of the direct wave without any reflections. This level was consistent with previous measurements of the output level of the sound source performed at greater depths, allowing better separation of the direct wave and the reflections.

The received signals at the other hydrophones were treated with a three-step processing to arrive at the calculated propagation loss for the decade band:

1. pulse compression in the frequency domain,
2. selection of a time segment around the compressed pulse in the time domain,
3. frequency averaging of the received level within the decade band.

The purposes of these three steps is to increase the apparent signal-to-noise ratio of the measurement, by discarding background noise data known to not be part of the transmitted signal. Contrary to the cross-correlation approach used for the reference hydrophone, this time-windowing in step 2 used a sufficiently long time segment to include the full reverberation of the compressed pulse. Finally, the propagation losses are calculated as the level differences between the received levels and the previously measured source levels of the transmitter. The calculated propagation losses are shown in fig. 2.

The measured propagation losses are compared with the simple “seabed critical angle” (SCA) propagation loss model². This model is composed of two parts, one with spherical spreading and one with cylindrical spreading. Writing the propagation loss N_{PL} in terms of the propagation factor

$$N_{PL} = -10 \log (Fr_0^2) \quad (1)$$

with $r_0 = 1$ m, the propagation factor is split into the spherical part F_s and the cylindrical part F_c . Each of these two parts has a low-frequency and a high-frequency approximation of the average interaction with the water surface (and the bottom) combined with the corresponding geometrical spreading function, expressed as

$$F_s = \frac{1}{r^2} \left(\sigma_{s,LF}^{-1} + \sigma_{s,HF}^{-1} \right)^{-1} \quad (2)$$

$$F_c = \frac{1}{rH} \left(\sigma_{c,LF}^{-1} + \sigma_{c,HF}^{-1} \right)^{-1}$$

where H is the water depth and r is the slant range, i.e. the distance between the water surface above the source and the receiver location. The four interaction terms can be expressed asⁱ

$$\sigma_{s,HF} = 2 \quad \sigma_{s,LF} = 4(kd)^2 \left(\frac{h}{r} \right)^2 \quad (3)$$

$$\sigma_{c,HF} = 2\Psi \quad \sigma_{c,LF} = 2(kd)^2 (\Psi - \cos(\Psi) \sin(\Psi))^2$$

using the seabed critical angle $\Psi = \arccos(c_w/c_p)$, the wavenumber $k = 2\pi f/c_w$, the receiver depth h , the source depth d , and the speed of sound in the water and substrate c_w respectively c_p .

The sound velocity profile (SVP) was measured both during the ship measurements and during the propagation loss measurements. In both cases the SVP was between 1501 m/s and 1506 m/s. For the SCA model, we have used a value of 1503 m/s for both occasions. To find the speed of sound in the bottom substrate, we performed a simple minimization of the model-to-measurement differences. This produced a value of 1507 m/s, corresponding to a critical angle of 4.2°. This is slightly softer than the recommended 5.7° for “very fine silt”⁵.

4 SOURCE LEVEL

The ship under test performed a total of seven transits during the trials, the first three in a slightly faster condition than the latter four. Technical staff onboard the ship under test monitored the operating condition to confirm that the ship operated with consistent engine power and speed thorough water in the passages in the same condition. In the first three transits, the ship was still accelerating while passing the measurement area, which is why a decision was made to measure in a slower condition.

ⁱWe use the more precise formula given in the final report from the MMP2 project, appendix B⁶.

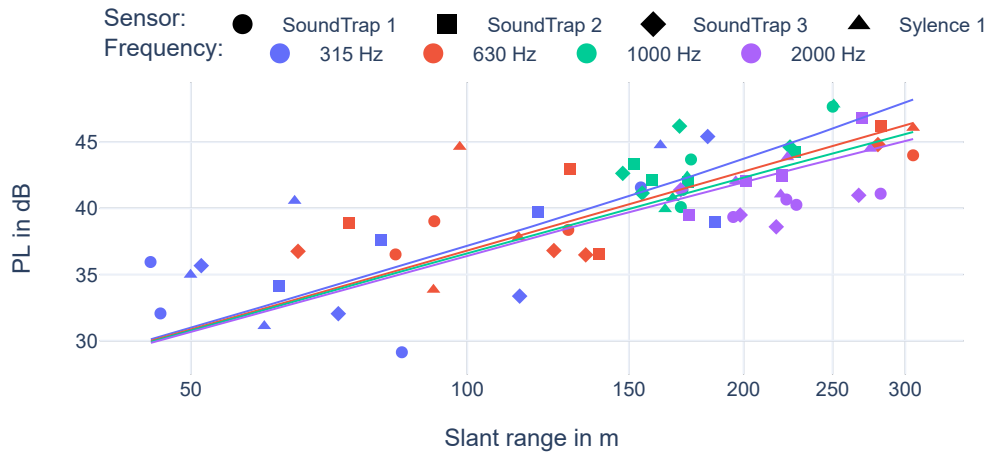


Figure 2: Measured and modeled propagation loss. Marks indicate measured PL to the different hydrophones, while lines are the model results. Colors indicate which frequency band the value concerns.

4.1 Analysis method

The calculation of the source level spectrum is performed mostly according to the recommended procedures by JASCO applied sciences⁵, with a few deviations. Data was selected for analysis in the time window when the ship was within $\pm 30^\circ$ of the closest point of approach (CPA), or a minimum of 30 s. This additional criteria of a minimum time is required for the closest hydrophones, where a $\pm 30^\circ$ window is transited very quickly. Within this data window, the power spectral density (PSD) was calculated using 5 s long processing windows, applying a Hann window and 50 % overlap for each processing window. This PSD was averaged within centidecade bands above 10 Hz giving a PSD $P_{i,h,j}(f)$ for each frequency band f , ship transit i , hydrophone h , and processing window j . These received PSD values are corrected for the background noise measured in between two transits, and PSD values less than 3 dB above the background noise were discarded from further analysis. The source level of the ship was computed separately for each of these processing windows, for each hydrophone used in the measurement, by applying the propagation model described in section 3. To compute the presented source levels, these intermediate values were power-averaged over the processing windows j and hydrophones h , and level averaged over the ship transits i .

To investigate how the results change when placing sensors unusually close to the measurement track, we have calculated the ship source level from different selections of the hydrophones, effectively forming “sub-arrays” with different geometries. In this study we chose five such sub-arrays to analyze, in addition to analyzing all sensors together. See table 2 for details on the sensor selection and labels for the arrays.

4.2 Results

The source levels for each transit as calculated from all hydrophones are shown in fig. 3. A detailed view of the tonal components in the low frequency range is shown in fig. 4. These figure show that the results for the four later transits in the slower speed have a very small spread, whilst the results in the faster speed are not as consistent. The average source levels of all transits in each speed are shown in fig. 5.

Table 2: The hydrophone selection of the analyzed sub-arrays.

Label	Hydrophones
Cable array	Colmar 1, Colmar 2
Distant array	Sylence 2, SoundTrap 4
Middle array	SoundTrap 2, SoundTrap 3
Near bottom array	Sylence 1, SoundTrap 1, SoundTrap 2
Far bottom array	SoundTrap2, Colmar 1, Sylence 2

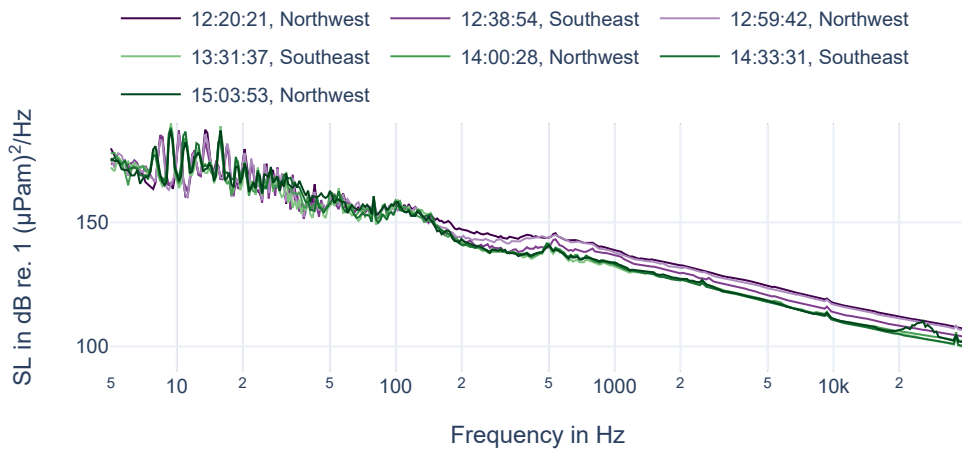


Figure 3: Source level for each ship transit, computed as the average between all hydrophones.

The spectra at high frequencies, above 500 Hz, follow a $-20 \log_{10}(f)$ slope, the slower speed around 4 dB lower than the fast speed. At frequencies between 50 Hz and 500 Hz the two spectra are very similar. The two spectra have very similar magnitudes at lower frequencies, but the distinct tonal components from the blade pass cavitation are shifted to slightly lower frequencies for the slower speed, as expected.

Focusing on the source levels calculated from the four transits in the slower speed, the results from the different sub-arrays presented in table 2 are shown in fig. 6, and the corresponding differences from the average of all hydrophones are shown in fig. 7. Looking first at the high frequencies, above 500 Hz, the largest differences are found in the “Distant array” and the “Middle array”, i.e., the source level computed from the vertical arrays with two autonomous hydrophones at 220 m and 70 m respectively from the measurement track. These differences are 2 dB lower from the “Distant array” and 2 dB higher from the “Middle array”. In the frequency range between 20 Hz and 50 Hz, the differences are mainly caused by the higher calculated source level from the Colmar hydrophones, which are the only hydrophones on the south-west side of the measurement track. Below 20 Hz the differences are larger and somewhat more erratic. This frequency range is very influenced by the Lloyd mirror effect, giving both a worse signal to noise ratio and an larger uncertainty in the propagation loss.

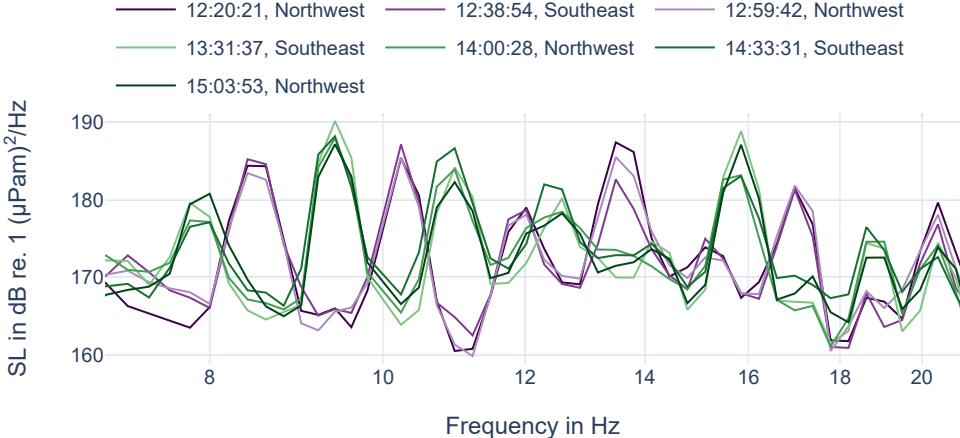


Figure 4: Detailed source level for each transit in the lower frequency range.



Figure 5: Average source level of all hydrophones and all transits, for the two speeds measured.

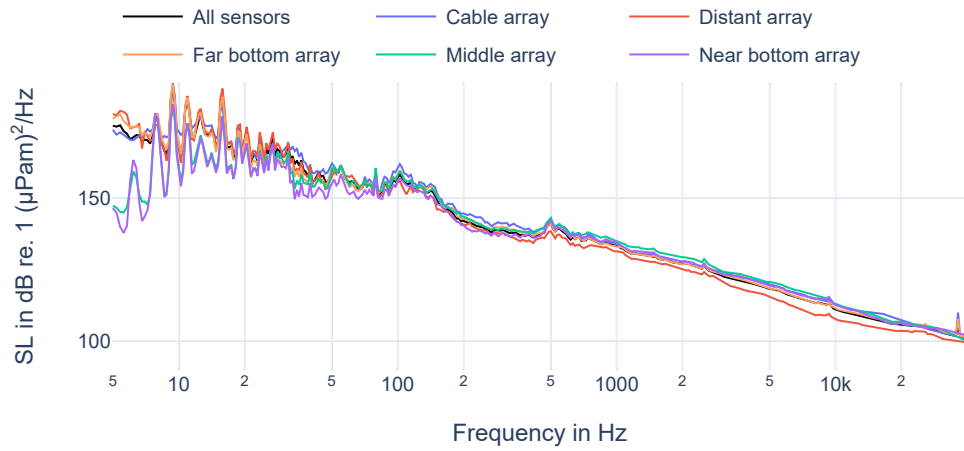


Figure 6: Source levels for the slower transits, as calculated from the sub-arrays defined in table 2.

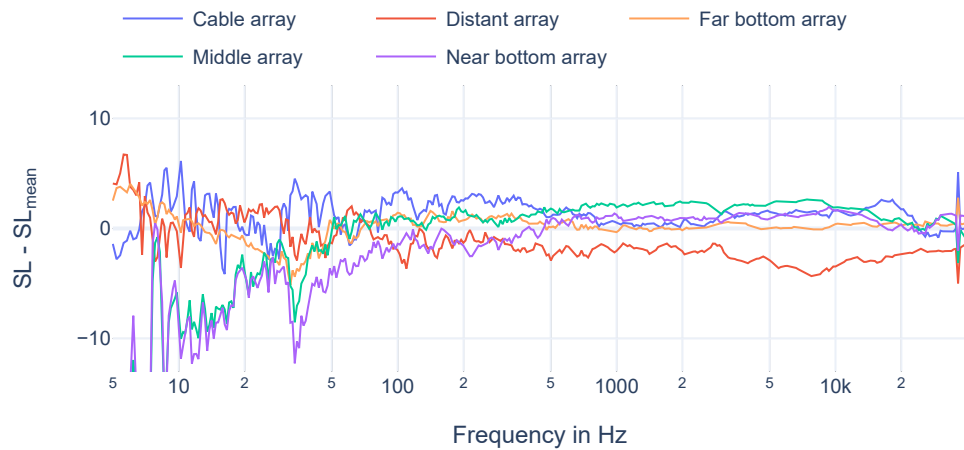


Figure 7: Difference in computed source levels for the slower transits, comparing the sub-arrays defined in table 2 with the average of all hydrophones.

5 DISCUSSION

The measured propagation loss has a somewhat large spread, with a 3 dB root mean square deviation from the propagation model. Unfortunately the measurement scheme clustered the high frequency chirps at farther ranges, which limits the insights that can be drawn from this measurement. It would also have been interesting to perform measurements at lower frequencies that are more influenced by Lloyd mirror effects or seabed cutoff effects, both which mainly impact frequencies lower than the 315 Hz decidecade band⁷. The optimization for the compressional wave speed in the seabed substrate yielded a very soft bottom. During the measurements of the ship source level, several large concrete blocks were used as anchors for the measurement vessel. When retrieved, these were covered in a thick layer of silt on top, indicating that they sunk substantially into the bottom. This unintentional sampling of the bottom substrate confirms that the bottom is very soft, but the exact acoustical properties can of course not be known. Since the measurements indicate such a soft bottom, the propagation model will almost be the same as a deep ocean model accounting for Lloyd mirror effects. As such, these measurements give little insight into the accuracy of the propagation model in general.

The level differences between the sub-arrays analyzed in this work are overall small in the high frequency range, above say 100 Hz. This is an indication that it is feasible to measure with close sensors for this high frequency range. In the range from 30 Hz to 50 Hz there are much larger differences. There are two likely sources for these differences: propagation loss and source near fields. The wavelength at these frequencies is between 30 m and 50 m, which is in the same order as much of the measurement geometry, which is often a domain where complicated interactions can occur. With the knowledge available for these measurements it is very difficult to judge the correct source level in this frequency range. It would be of interest to repeat this style of measurement in more settings and with a fuller understanding of the low frequency propagation conditions.

REFERENCES

1. ISO. Requirements for measurements in shallow water. Technical Report 17208-3:2023, DRAFT.
2. Alexander O. MacGillivray, S. Bruce Martin, Michael A. Ainslie, Joshua N. Dolman, Zizheng Li, and Graham A. Warner. Measuring vessel underwater radiated noise in shallow water. *The Journal of the Acoustical Society of America*, 153(3):1506–1524, mar 2023. ISSN 0001-4966. doi: 10.1121/10.0017433.
3. ISO. Requirements for precision measurements in deep water used for comparison purposes. Technical Report 17208-1:2016, 2016.
4. Bureau Veritas. Underwater Radiated Noise. Technical Report NR614, 2018.
5. David E. Hannay, Michael A. Ainslie, Krista B. Trounce, Justin Eickmeier, Alexander O. MacGillivray, S. Bruce Martin, and Veronique Nolet. Recommended Procedures for Measuring URN Noise Emissions of Ships, for Quiet Ship Certification. Technical Report 03129, JASCO Applied Sciences, September 2023.
6. Alexander MacGillivray, S. Bruce Martin, Michael A. Ainslie, Joshua N. Dolman, Zizheng Li, Graham A. Warner, Carmen B. Lawrence, Federica Pace, Max Schuster, and Dietrich Wittekind. Towards a Standard for Vessel URN Measurement in Shallow Water. Technical Report 02427, JASCO Applied Sciences, May 2022.
7. Finn B. Jensen, William A. Kuperman, Michael B. Porter, and Henrik Schmidt. *Computational Ocean Acoustics*. Springer New York, 2 edition, 2011. ISBN 978-1-4939-3704-2.